© IWA Publishing 2019
614

Water Practice & Technology Vol 14 No 3
doi: 10.2166/wpt.2019.047

Surface grafting of polyvinyl alcohol (PVA) cross-linked with glutaraldehyde (GA) to improve resistance to fouling of aromatic polyamide thin film composite reverse osmosis membranes using municipal membrane bioreactor effluent

Godwill Kasongo, Chad Steenberg, Bradley Morris, Gracia Kapenda, Nurah Jacobs and Mujahid Aziz*

Faculty of Engineering, Department of Chemical Engineering, Cape Peninsula University of Technology, Bellville 7435, South Africa

*Corresponding author. E-mail: azizm@cput.ac.za

Abstract

Membrane surface modification is a favourable method to handle fouling during wastewater treatment processes. In this study, grafting of polyvinyl alcohol (PVA) through cross-link with Glutaraldehyde was applied to a thin film composite reverse osmosis membrane to enhance the resistance to flux decline. The analytical analyses attenuated total reflectance Fourier transform infrared spectroscopy (ATR-FTIR) and scanning electron microscopy were performed to evaluate the impact of surface modification. Biofouling using *Escherichia coli* (*E. coli*) bacterial solution and fouling tests using a bench scale reverse osmosis system with a simulated secondary effluent from a membrane bioreactor were used to assess the impact of the surface modification initiated on antifouling properties of the membrane. It was shown that the morphological structure and the chemical properties of the membrane were altered, whereas the pure water flux slightly decreased after modification. Although a slight decrease of salt rejection was observed, the membrane resistance to fouling improved and the biofouling model used revealed the anti-biofouling capacity of the membrane. The flux decline and flux recovery ratios improved with an increase in PVA concentration. The sterilization ratio increased from 33.8 to 36.8% and the pure water flux decline decreased from 46.04 to 25.94% after modification.

Key words: fouling, grafting, MBR secondary effluent, membrane surface, reverse osmosis membrane, water reuse

INTRODUCTION

Currently, the reverse osmosis (RO) process is most commonly used to meet the high demand for good water quality for water reuse in large municipalities (Yu *et al.* 2017). However, contaminants present in the effluent being treated adsorb to the surface of the membrane and causes it to foul (Tang *et al.* 2014). Despite the extensive application and advantages of the RO process, a major challenge remains: membrane fouling. This has a negative effect on the performance of the system, resulting in flux and product quality decline (Zhao *et al.* 2010); high energy consumption (Tang *et al.* 2016); and a decrease of membrane life span (Yu *et al.* 2017). The extent of RO membrane fouling depends on the quality of the influent (Khan *et al.* 2014), where fouling during wastewater treatment is more complex than sea water treatment (Tang *et al.* 2016). Fouling on RO membranes is due to scaling by inorganics; adhesion and growth of bacteria onto the surface; and a cake layer formed by colloids and interactions between organics (Tang *et al.* 2014). These mechanisms may occur concurrently (Liu *et al.* 2015).

Water Practice & Technology Vol 14 No 3
doi: 10.2166/wpt.2019.047

Aromatic polyamide (PA) thin-film composite (TFC) RO membranes are commonly used for desalination and the treatment of wastewater due to its high performance of salt rejection and permeability (Liu *et al.* 2015). As a result of surface properties such as chemical structure; surface roughness; charge; hydrophilicity and limited stability to chlorine-based disinfectants, they are prone to fouling (Zhang *et al.* 2017). Remedial action to minimize fouling includes the following: pretreatment of feed solution; cleaning of the membrane by physical or chemical methods; and membrane surface modification (Asadollahi *et al.* 2017). Pretreatment and cleaning techniques can be costly (Hu *et al.* 2016), whereas surface modification through membrane coating or grafting negates this (Sun *et al.* 2013). During grafting, the physicochemical properties of the membrane surface are easily and permanently altered due to the simplicity of the method and the high grafting yield, which is sustainable (Asadollahi *et al.* 2017). The grafting method consists of introducing polar groups or hydrophilic monomers to the surface of the membrane, applying one of the following: plasma treatment, UV-irradiation or chemical treatment (Saqib & Aljundi 2016).

During the chemical modification of a PA TFC membrane surface, quaternary ammonium cations and salicylaldimines were introduced through amidation and condensation reactions. The membrane structure was investigated with instrumental and chemical analysis. The modified membranes were positively charged, with an increase in water flux and a slight decrease in salt rejection, with lower contact angles than the unmodified membranes. Anti-biofouling tests using an *E. coli* bacteria solution indicated resistance to microbial adhesion for the modified membranes (Zhang *et al.* 2017). In a previous study, Cheng *et al.* (2013) used the protein bovine serum albumin (BSA) to conduct fouling tests after grafting of N-isopropyl acrylamide (NIPAm) and acrylic acid (AA). The flux decline of the unmodified and modified membranes was about 45.3% and 20.7% after 40 h filtration time respectively, showing an enhanced fouling resistance to BSA. Modifications through grafting conducted by various researchers have altered membranes' physiochemical and permeation properties differently. Induced grafting by carbodiimide with poly(ethylene glycol) derivatives (Kang *et al.* 2011) and induced grafting carbodiimide with imidazolidinyl urea (Xu *et al.* 2013) were performed on a PA TFC RO membrane. In both studies, the membrane hydrophilicity increased, but pure water flux decreased. However, salt rejection only decreased with the grafting of imidazolidinyl urea. A facile modification approach was applied to a commercial TFC RO membrane to improve membrane antifouling properties where the membrane was treated with aqueous glutaraldehyde (GA) and by polyvinyl alcohol (PVA) aqueous solution (Hu *et al.* 2016). Modification of these membranes caused an increase in membrane roughness and hydrophilicity, however, the salt rejection and resistance to foulants were improved by changing the concentration of PVA in the modifying solution. The performance of the membranes was also evaluated using an industrial effluent from a textile factory where the rejection and resistance to fouling were examined. During this study, the flux declines ratio (FDR) decreased from 34.9% to 21.4%, after modification. According to past studies (An *et al.* 2011), PA TFC RO membranes after surface modification with PVA indicated better performance. However, no studies have been done with PVA cross-linked with GA as a grafting solution to evaluate resistance to fouling using a domestic municipal secondary membrane bioreactor (MBR) effluent.

In this study, we investigated the resistance to fouling of a low-pressure PA TFC RO membrane in the treatment of a simulated domestic municipal secondary effluent from an MBR with a lab scale RO flat cell. PVA grafting solutions were used as modifying agents (Na *et al.* 2000) where it is an additive with good hydrophilicity (Ma *et al.* 2007) and anti-fouling properties (Tang *et al.* 2009). Scanning electron microscopy (SEM) and attenuated total reflectance Fourier Transform infrared spectroscopy (ATR–FTIR) analysis were conducted to study the structure of the unmodified and modified membranes.

Water Practice & Technology Vol 14 No 3
doi: 10.2166/wpt.2019.047

METHOD

Materials and reagents

A commercial spiral wound PA TFC RO membrane obtained from Dow Chemical Company was used as a virgin membrane. PVA, GA, sodium chloride, potassium chloride, dipotassium phosphate, sodium bicarbonate, potassium phosphate, magnesium sulphate, calcium sulphate, humic acid, sulfuric acid and ammonium phosphate were all purchased from Sigma Aldrich (Pty) Ltd, South Africa. All chemicals were of analytical grade and used without further purification. Nutrient agar (NA), nutrient broth (NB) and petri dishes were obtained from Lasec SA (Pty) Ltd. *Escherichia coli* ATCC 11303 strains were purchased from LGC Standards SA. Deionized (DI) water with of an electrical conductivity lower than 10 μs/cm was used for all solution preparation as well as membrane rinsing, from a Millipore water purification system; and further sterilized at 121 °C in the autoclave for solution preparation during biofouling experiments.

Modification of the virgin membrane

Grafting of PVA

PVA was grafted onto the surface of the virgin membrane through covalent bonding initiated by GA (Figure 1). Membrane sample 18 cm in length and 12 cm in width (Hu *et al.* 2016) was immersed in DI water over a period of 12 hours, replacing the water hourly to remove preservatives from the membrane sample. DI water was used to thoroughly rinse the membrane and allowed it to dry at room temperature. The membrane was then wrapped around a rectangular frame, in such a way that the layer faced the inner part of the frame to allow full contact with the modifying agent solution. The GA solution purchased from the manufacturer was diluted from 25 wt% to 0.05 wt%. A 100 mL of the prepared solution was added into the rectangular frame where the membrane has been fixed for 5 min and the excess solution removed. The membrane was rinsed with DI water and allowed to dry completely. PVA solutions were prepared at the following concentrations; 0.5 $g.L^{-1}$, 0.1 $g.L^{-1}$, 0.15 $g.L^{-1}$ and 0.2 $g.L^{-1}$. A fixed amount of PVA was added to 1 L of DI water and placed on a heating element with a magnetic stirrer to mix the solution for 30 min at 75 °C until the PVA was dissolved completely. The PVA solution was allowed to cool and the pH was adjusted to 3.05 using diluted sulphuric acid. The prepared PVA solution was then poured on the coated membrane around the rectangular frame for 3 min, and the solution was removed and placed in the oven at 50 °C for 6 min. DI water was used to rinse the modified membrane, and the membrane was placed in DI water at 45 °C for at least 10 hours, replacing the water hourly to remove unreacted molecules from the surface. The membrane was stored in DI water for experimental fouling test and structure analysis.

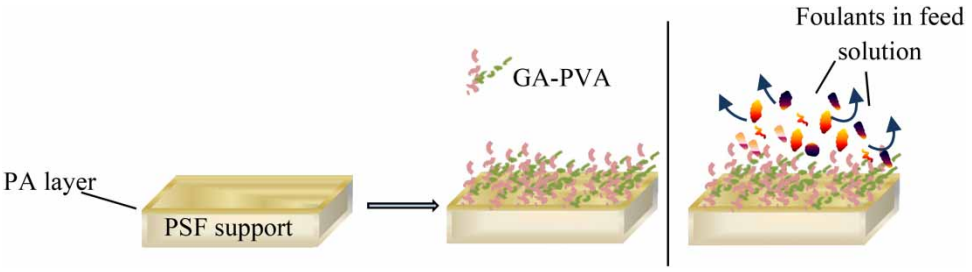

Figure 1 | Graphic illustration of the modification procedure.

Water Practice & Technology Vol 14 No 3
doi: 10.2166/wpt.2019.047

Characterization of the modified and unmodified membrane

A Thermo Scientific Nicolet iS10 instrument was used with an ATR accessory to observe the chemical structure of the membrane after modification. The internal reflecting element was a diamond crystal. Spectra were collected in the range 4,000–650 cm^{-1} with 64 scans and a resolution of 4 cm^{-1}. Spectra were corrected for atmospheric background and baseline corrected.

The surface morphology of both modified and unmodified membranes were observed by scanning electron microscope (SEM) using a Nova NanoSEM instrument. Top view images of the surfaces were scanned and compared at 40,000× magnification and 5.00 keV landing E, and cross-section was scanned at 1,000× magnification and 5.00 keV landing electron.

Membrane performance and anti-fouling evaluations

All experimental runs were carried out on a lab scale crossflow SEPA CF II RO cell unit. The synthetic feed solution consisted of identified foulants of simulated a secondary effluent from a municipal wastewater treatment plant as described by Giannakis *et al.* (2013) and Rivas *et al.* (2015) (Table 1). A hydra-cell pump (model: G20BDSTHFECG) was used to pump the feed from a stainless steel tank to the RO cell and permeate was collected while the brine was recycled back to the tank. LabVIEW was used to set and monitor the operating conditions of the system. The membranes in the cell were flushed with DI water (≈5 μS/Cm) overnight at 5 bar feed pressure and 19 cm/s cross flow velocity prior to experiments, and the DI water flux of membranes was measured and compared. The trans-membrane pressure was regulated and kept constant throughout the 42 hr. experimental run, also at 5 bar feed pressure, 19 cm/s cross flow velocity and ambient temperature. Time-dependent flux, as well as streams electroconductivity (EC) and total dissolved solids, were recorded at 45 min intervals.

Table 1 | Synthetic feed solution composition

Chemical composition	Concentration (mg/L)
Potassium chloride	4
Dipotassium phosphate	7
Sodium chloride	7
Sodium bicarbonate	93
Magnesium sulphate	60
Ammonium sulphate	60
Calcium sulphate	60
Humic acid	5

The flux and observed salt rejections were calculated according to Hu *et al.* (2016) Equation (1) and Zhang *et al.* (2017) Equation (2) respectively:

$$J = \frac{V}{A \times \Delta T} \tag{1}$$

$$R = \frac{C_f - C_p}{C_f} \times 100 \tag{2}$$

In Equation (1) V, A, ΔT and J were the volume of permeate (L), the effective area of the membrane (m^2), the interval time (hr) and the permeate water flux respectively. In Equation (2) C_f (μS/cm), C_p (μS/cm) and R (%) were the feed conductivity permeate conductivity and salt rejection,

Water Practice & Technology Vol 14 No 3
doi: 10.2166/wpt.2019.047

respectively. EC was measured using a conductivity meter (YSI EcoSense EC300, YSI Inc., USA). After the experimental runs, fouled membranes were flushed with DI water at the same initial conditions and the DI water flux re-evaluated. Fouling was evaluated by measuring the flux decline ratio and flux recovery ratio of the membranes.

$$FDR = \left(\frac{J_i - J_t}{J_i}\right) \times 100 \tag{3}$$

$$FRR = \left(\frac{J_{wi}}{J_{wf}}\right) \times 100 \tag{4}$$

In Equation (3) FDR (%) is the flux decline ratio, J_i and J_t are the initial flux of water and time-dependent flux of water (in $L.m^{-2}\,h^{-1}$), respectively. In Equation (3) FRR is the flux recovery ratio (%), J_{wi} and J_{wf} ($L.m^{-2}\,h^{-1}$) are the flux of pure water (DI water) before and after fouling experiment, respectively.

Membrane anti-biofouling evaluation

Anti-biofouling properties of membranes were evaluated in terms of resistance to bacterial growth and biofilm formation. *E. coli* bacterial solution was used as a model foulant. Bacterial growth measurement was similar to that described by Wang *et al.* (2015) with minor modifications. The membrane was cut into small sizes (2 cm × 2 cm) and placed under UV for half hour. Thereafter, it was placed in contact with NB ≈ 0.47 OD (590 nm) containing *E. coli* suspension, for 3 hours. The membrane was then removed and rinsed with fresh broth and the solution collected was diluted in series (2–10 fold). 100 μL of each dilution were plated on NA medium and placed in the incubator at 37°C overnight. The plate count method was used to determine the number of *E. coli* bacteria in contact with the membrane. The NB of *E. coli* suspension, without being in contact with the membrane, was also diluted and incubated as above. The number of *E. coli* bacteria without being in contact with the membrane was also determined as mentioned above, and this allowed for the calculation of the mortality ratio (R):

$$R = \left(\frac{B - A}{A}\right) \times 100 \tag{5}$$

Where is B the number of viable bacteria not in contact with the membrane surface and A is the number of viable bacteria in contact with the membrane surface for given contact time. Biofouling effect was further investigated by measuring pure water flux of membranes before and after incubation of 2×10^8 $CFU.mL^{-1}$ *E. coli* bacteria suspension for 30 hours.

RESULTS AND DISCUSSION

Membrane characterization

The ATR-FTIR was used to analyse membrane surface functional groups and illustrated that grafting succeeded. The peaks at 1,240, 1,482, 1,510 and 1,589 cm^{-1} in Figure 2 (left and right) are characteristics of the polysulfone support layer of the membrane, as described by Wei *et al.* (2010) and Cheng *et al.* (2013). The small but clear peaks at 1,610 cm^{-1} of membranes spectra in both figures correspond to the amide I group (C = O stretching), which was ascribed to the polyamide top layer of the membrane (Liu *et al.* 2015). The presence of these peaks showed that the structures of the membranes were not affected after modification (Lin *et al.* 2016). The spectra of PVA modified membranes

Water Practice & Technology Vol 14 No 3
doi: 10.2166/wpt.2019.047

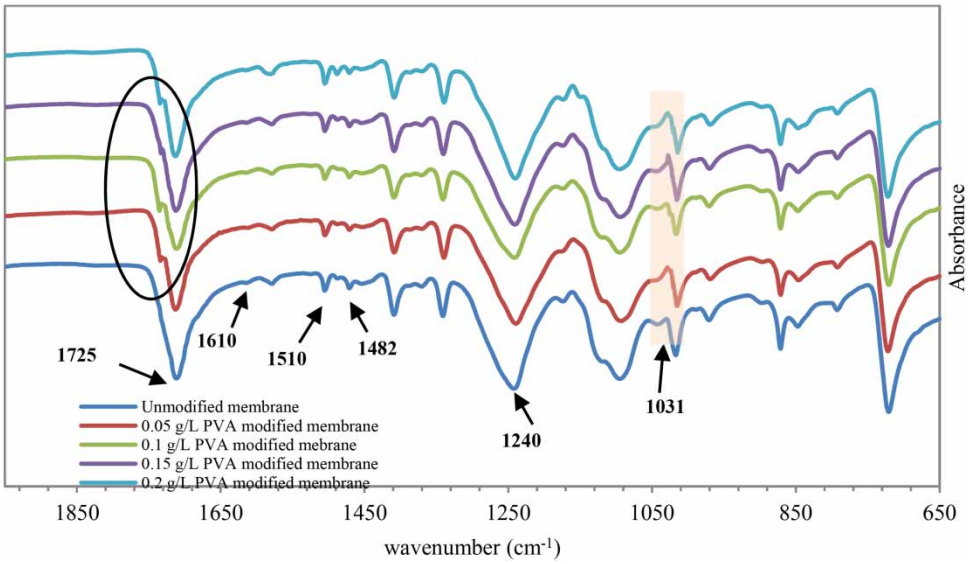

Figure 2 | ATR-FTIR spectra of unmodified and PVA modified membranes.

show an adsorption band at about 1,725 cm^{-1} attributed to the presence of PVA molecules attached to the polyamide layer (Hu *et al.* 2016). The bend of the peak at about 1,030 cm^{-1} on the modified membranes spectra shows the cross-linkage of the PVA molecules and GA onto the surface of the membrane (Tang *et al.* 2016).

Membrane morphology and structure were investigated using SEM. Top views of all membranes in Figures 3 and 4 present ridge and valley surface structure for all membranes (Freger *et al.* 2002). PVA modified demonstrated denser surface as compared to the unmodified membrane. The level of disproportion in the structure differed with a change in concentration of the modifying agent. PVA modified membranes became more compact as the concentration of PVA increased from 0.05 to 0.2 g/L, causing a surface negative charge decrease (Hu *et al.* 2016). Modifications conducted by other researchers (An *et al.* 2011) showed that a less dense surface ensued smoothness; while the use of GA and PVA caused denser surfaces, hence roughness. Cross-section images of PVA modified membranes in Figure 3 demonstrated the impact of the modification on the surface of the membrane. The thickness

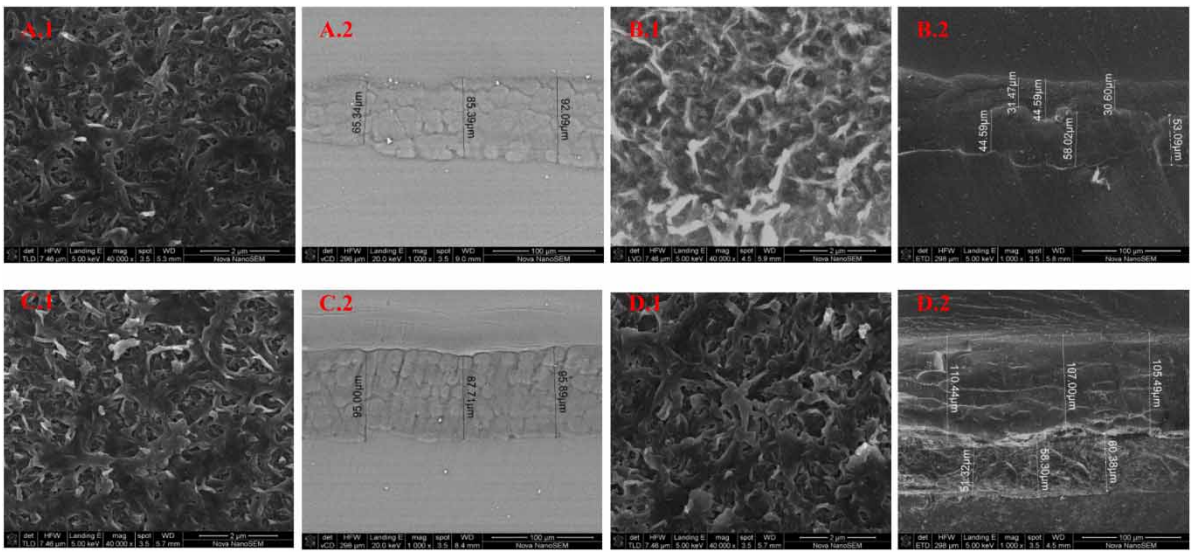

Figure 3 | SEM images of PVA modified membranes (top view & cross-section): (A) 0.05 $g.L^{-1}$ PVA, (B) 0.1 $g.L^{-1}$ PVA, (C) 0.15 $g.L^{-1}$ PVA and (D) 0.2 $g.L^{-1}$ PVA.

Water Practice & Technology Vol 14 No 3
doi: 10.2166/wpt.2019.047

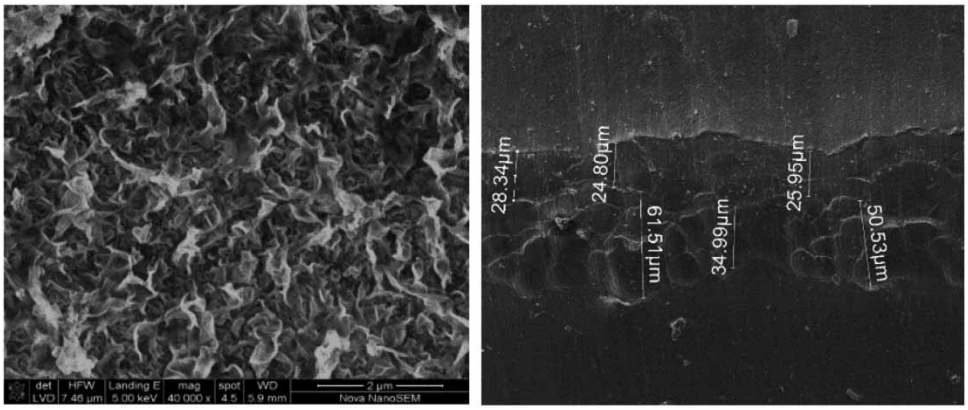

Figure 4 | SEM images of the virgin membrane: top view (Left) & cross-section (Right).

of the top selective layer of membrane increased with an increase in PVA concentration. Modifications of membranes using PVA resulted in an increase of the thickness of the selective skin layer of the TFC membrane as the modifying solution concentration increased.

Membrane permeation and salt rejection

Membrane permeation was tested using pure water at 5 bar feed pressure and 19 cm/s cross (Table 2). Figure 5 displays the time-dependent flux of the 0.05 g/L, 0.1 g/L and 0.15 g/L PVA modified membranes compared to the time-dependent flux of the unmodified membrane. The observed salt rejection was tested using the simulated secondary effluent from an MBR. Pure water flux of PVA modified membranes decreased with increasing PVA concentration in the modifying solutions. This could be explained by an increase in hydraulic resistance of the membranes (Liu *et al.* 2015). This resistance disturbs the normal hydrophilicity nature of the membrane (Azari & Zou 2012). The salt rejection decreased slightly for both modifications with an increase in the modifying agent concentration. This could be due to the membrane surface charge and the interactions of the ions between the membrane surface and the foulants after grafting (Yu *et al.* 2013). The decrease in salt rejection for both investigations could also be attributed to the Donnan exclusion effects (Cheng *et al.* 2013).

Table 2 | Values of pure water flux (initial and final) of the modified membranes and the observed salt rejection during filtration of the synthetic feed solution (grafting of PVA)

Membrane	The initial flux of pure H_2O ($L.m^{-2}\,h^{-1}$)	The final flux of pure H_2O ($L{\cdot}m^{-2}\,h^{-1}$)	Salt rejection (%)
Unmodified membrane	62.29	42.51	87.74
0.05 g/L PVA membrane	52.05	38.50	87.79
0.1 g/L PVA membrane	49.07	37.76	87.09
0.15 g/L PVA membrane	48.66	39.45	84.54
0.2 g/L PVA membrane	38.48	30.49	80.65

Fouling test

Figure 6 displays the time-dependent flux of the modified membranes compared to the unmodified membrane during the filtration of the synthetic feed solution. Same operating conditions with initial permeate flux of 57.5 $L.m^{-2}.h^{-1}$, 19 cm/s cross flow velocity, and 5 bar pressure were used for all experimental runs. The flux was normalized at 25°C.

Water Practice & Technology Vol 14 No 3
doi: 10.2166/wpt.2019.047

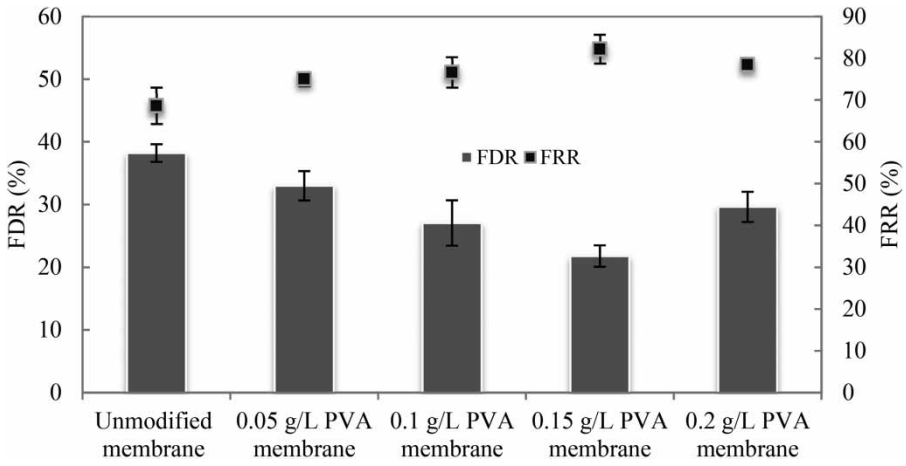

Figure 5 | FDR during filtration of the synthetic feed and pure water FRR of membranes.

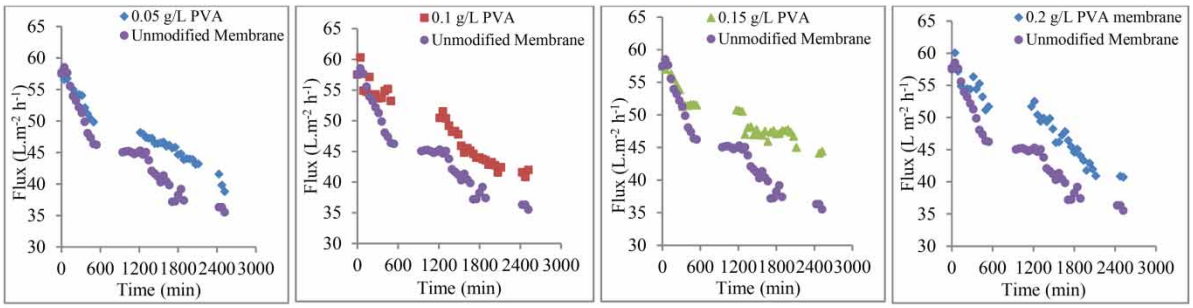

Figure 6 | Time-dependent flux of unmodified and PVA modified membranes (Bottom) during filtration of the synthetic feed.

The persistent decrease in the normalized flux, for all graphs in Figure 6, proved the presence of fouling (Cheng *et al.* 2013). Over time the flux decline is more noticeable, and the flux difference between the unmodified and the modified membranes, increases. The distance between fluxes curves on each plot differ. The normalized flux of modified and unmodified membranes seemed to be similar in the first 500 min; thereafter the difference was more noticeable. The unmodified membrane flux declined the most. Among PVA modified membranes, the 0.15 g/L PVA membrane decline the least. Flux decline rate indicates of fouling severity, thus higher flux decline indicated that sever fouling happened (Yu *et al.* 2013). Thus it can be deduced that the fouling was more severe with the unmodified membrane and the less with modified membranes, with increasing concentration. It is known that the reduction in flux decline after modification is due to the lower hydraulic resistance to water permeation of the surface of the membrane where the fouling layer is formed (Yu *et al.* 2013). Thus it can be said that PVA modified membrane permitted the formation of a lower hydraulic resistance at the surface of the membrane during filtration.

Antifouling properties of the membranes were evaluated using the FDR and the FRR as reported by other studies Zhao and Chen (2015) and Shen *et al.* (2017). The FRR also revealed the cleaning properties of membranes after fouling. The highest FDR and lowest FRR were obtained from the unmodified membrane. The FDR was 38.21% before modification while the lowest value of the FDR was 21.78% among PVA modified membranes. The lower flux decline rate shows that the membrane possessed better resistance to fouling (Hu *et al.* 2016). The pure water flux of the unmodified membrane after fouling experiments was recovered only to 68.61%, while the FRR of PVA modified membranes were higher, and increasing with an increase in the concentration of the modifying solutions. Higher flux recovery indicates that fouling is more reversible (Mahdavi *et al.* 2017). Thus it

Water Practice & Technology Vol 14 No 3
doi: 10.2166/wpt.2019.047

can be said that fouling of modified membranes was more reversible with increasing concentration of the modifying agents up to 0.15 g/L PVA.

Membrane anti-biofouling properties

The 0.1 g/L PVA modified membrane and the unmodified membrane were selected to perform biofouling testing and evaluate membrane anti-biofouling properties using an *E. coli* bacterial solution. The *R* value of the 0.1 g/L PVA modified membrane was 36.75%, whilst the *R* value of 33.80% was obtained for the unmodified membrane. A higher sterilization ratio shows that the membrane possesses antimicrobial properties, obstructing multiplication of microorganisms in the tests (Zhang *et al.* 2013).

The unmodified and 0.15 g/L PVA modified membranes were further tested for water flux in the RO process after exposure to *E. coli* bacteria cell suspension for 30 hours, and values are reported in Figure 7. Pure water flux of the membranes was measured at the same initial conditions and compared. R values of the both unmodified and 0.1 g/L PVA modified membranes were similar, showing the similar capacity to obstruct reproduction of microorganisms; results presented in Table 3, however, showed that the PVA modified membrane had a higher resistance to adhesion of microorganisms to the surface of the membranes.

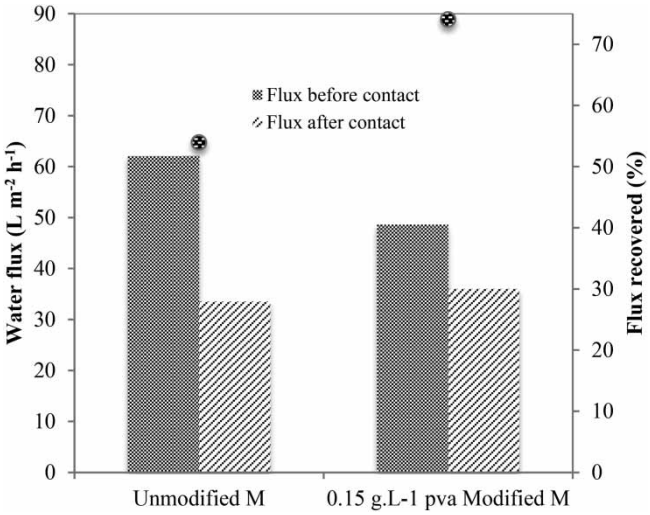

Figure 7 | Pure water flux of membranes before and after the biofouling of *E. coli* bacteria.

Table 3 | Values of membrane sterilization ratios obtained from the selected membranes

Membrane	A ($\times 10^6$ CFU/mL)	B (CFU/mL)	Sterilization ratio, R (%)
Unmodified membrane	106	16×10^7	33.75
0.1 g/L PVA modified M	100	16×10^7	36.80

The water flux of the unmodified membrane decreased from 62 to 34 L.m^{-2} hr^{-1}; while the selected PVA modified membrane decreased from 49 to 36 L.m^{-2} hr^{-1}. It implies that the flux of the unmodified membrane was recovered to only 54%, while the flux of the PVA modified membrane flux was recovered to 74%, thus showing poor adhesion of micro-organisms on the modified membranes.

CONCLUSION

Cross-linkage of GA and PVA was successfully grafted onto the active layer of the TFC RO membrane surface. The chemical structure of unmodified and modified membranes was determined by chemical

Water Practice & Technology Vol 14 No 3
doi: 10.2166/wpt.2019.047

analysis. ATR-FTIR spectra revealed noticeable new peaks as well as an increase in their intensities highlighting the successful grafting on the membrane surface. Top view SEM images clearly show a change in density whereas cross-section SEM images show changes in the thickness of the top layers of the modified membranes. This top layer thickness increases with the increase of grafting solution concentration. Pure water flux of PVA modified membranes varied in descending order with an increase of the grafting solution concentration. The flux decline ratio decreases and flux recovery ratio increases for the modified membranes as grafting solution concentration, increases. During the biofouling test with *E. coli* bacterial solution, the sterilization ratio increased after modification. In conclusion, these modified membranes showed high resistance to fouling and great potential as an RO purification step for municipal secondary MBR effluent.

ACKNOWLEDGEMENTS

We thank the Biotechnology Laboratory of CPUT Cape Town for providing with the necessary equipment and material and environment to conduct for assisting during biofouling tests.

REFERENCES

An, Q., Li, F., Ji, Y. & Chen, H. 2011 Influence of polyvinyl alcohol on the surface morphology, separation and anti-fouling performance of the composite polyamide nanofiltration membranes. *Journal of Membrane Science* **367**(1–2), 158–165. https://doi.org/10.1016/j.memsci.2010.10.060.

Asadollahi, M., Bastani, D. & Musavi, S. A. 2017 Enhancement of surface properties and performance of reverse osmosis membranes after surface modification: a review. *Desalination* **420**, 330–383. https://doi.org/10.1016/j.desal.2017.05.027.

Azari, S. & Zou, L. 2012 Using zwitterionic amino acid l-DOPA to modify the surface of thin film composite polyamide reverse osmosis membranes to increase their fouling resistance. *Journal of Membrane Science* **401**, 68–75.

Cheng, Q., Zheng, Y., Yu, S., Zhu, H., Peng, X., Liu, J. & Gao, C. 2013 Surface modification of a commercial thin-film composite polyamide reverse osmosis membrane through graft polymerization of N-isopropylacrylamide followed by acrylic acid. *Journal of Membrane Science* **447**, 236–245. https://doi.org/10.1016/j.memsci.2013.07.025.

Freger, V., Gilron, J. & Belfer, S. 2002 TFC polyamide membranes modified by grafting of hydrophilic polymers: an FT-IR/AFM/TEM study. *Journal of Membrane Science* **209**, 283–292.

Giannakis, S., Isabel, A., Gamo, M., Darakas, E. & Escalas-can, A. 2013 ScienceDirect Impact of different light intermittence regimes on bacteria during simulated solar treatment of secondary effluent: implications of the inserted dark periods. *Solar Energy* **98**, 572–581. https://doi.org/10.1016/j.solener.2013.10.022.

Hu, Y., Lu, K., Yan, F., Shi, Y., Yu, P., Yu, S. & Li, S. 2016 Enhancing the performance of aromatic polyamide reverse osmosis membrane by surface modification via covalent attachment of polyvinyl alcohol (PVA). *Journal of Membrane Science* **501**, 209–219. https://doi.org/10.1016/j.memsci.2015.12.003

Kang, G., Yu, H., Liu, Z. & Cao, Y. 2011 Surface modification of a commercial thin film composite polyamide reverse osmosis membrane by carbodiimide-induced grafting with poly (ethylene glycol) derivatives. *Desalination* **275**(1–3), 252–259. https://doi.org/10.1016/j.desal.2011.03.007.

Khan, M. T., Busch, M., Molina, V. G., Emwas, A. H., Aubry, C. & Croue, J. P. 2014 How different is the composition of the fouling layer of wastewater reuse and seawater desalination RO membranes? *Water Research* **59**, 271–282. https://doi.org/10.1016/j.watres.2014.04.020.

Lin, S., Huang, H., Zeng, Y. & Zhang, L. 2016 Facile surface modification by aldehydes to enhance chlorine resistance of polyamide thin film composite membranes. *Journal of Membrane Science* **518**, 40–49. https://doi.org/10.1016/j.memsci.2016.06.032.

Liu, M., Chen, Q., Wang, L., Yu, S. & Gao, C. 2015 Improving fouling resistance and chlorine stability of aromatic polyamide thin- film composite RO membrane by surface grafting of polyvinyl alcohol (PVA). *Desalination* **367**, 11–20. https://doi.org/10.1016/j.desal.2015.03.028

Ma, X., Su, Y., Sun, Q., Wang, Y. & Jiang, Z. 2007 Enhancing the antifouling property of polyethersulfone ultrafiltration membranes through surface adsorption-crosslinking of poly (vinyl alcohol). *Journal of Membrane Science* **300**(1–2), 71–78.

Mahdavi, H., Hosseinzade, M. T. & Shahalizade, T. 2017 A polyamide thin-film composite membrane modified by Michael addition grafting of hyperbranched poly (amine ester). *Journal of Polymer Research* 1–11. https://doi.org/10.1007/s10965-017-1272-x

Na, L., Zhongzhou, L. & Shuguang, X. 2000 Dynamically formed poly (vinyl alcohol) ultrafiltration membranes with good anti-fouling characteristics. *Journal of Membrane Science* **169**(1), 17–28.

Water Practice & Technology Vol 14 No 3
doi: 10.2166/wpt.2019.047

Rivas, G., Carra, I., Sánchez, J. L. G., López, J. L. C., Malato, S. & Pérez, J. A. S. 2015 Applied catalysis B: environmental modelling of the operation of raceway pond reactors for micropollutant removal by solar photo-Fenton as a function of photon absorption. *Applied Catalysis B, Environmental* **178**, 210–217. https://doi.org/10.1016/j.apcatb.2014.09.015

Saqib, J. & Aljundi, I. H. 2016 Journal of water process engineering membrane fouling and modification using surface treatment and layer-by-layer assembly of polyelectrolytes: state-of-the-art review. *Journal of Water Process Engineering* **11**, 68–87. https://doi.org/10.1016/j.jwpe.2016.03.009.

Shen, L., Zuo, J. & Wang, Y. 2017 Tris(2-aminoethyl)amine in-situ modified thin-film composite membranes for forwarding osmosis applications. *Journal of Membrane Science* **537**, 186–201. https://doi.org/10.1016/j.memsci.2017.05.035.

Sun, W., Liu, J., Chu, H. & Dong, B. 2013 Pretreatment and membrane hydrophilic modification to reduce membrane fouling. *Membranes* 226–241. https://doi.org/10.3390/membranes3030226.

Tang, C. Y., Kwon, Y.-N. & Leckie, J. O. 2009 Effect of membrane chemistry and a coating layer on physiochemical properties of thin film composite polyamide RO and NF membranes: II. Membrane physiochemical properties and their dependence on polyamide and coating layers. *Desalination* **242**(1–3), 168–182.

Tang, F., Hu, H., Sun, L., Wu, Q. & Jiang, Y. 2014 Fouling of reverse osmosis membrane for municipal wastewater reclamation: autopsy results from a full-scale plant. *Desalination* **349**, 73–79. https://doi.org/10.1016/j.desal.2014.06.018.

Tang, F., Hu, H., Sun, L., Sun, Y., Shi, N. & Crittenden, J. C. 2016 Fouling characteristics of reverse osmosis membranes at different positions of a full-scale plant for municipal wastewater reclamation. *Water Research* **90**, 329–336. https://doi.org/10.1016/j.watres.2015.12.028.

Wang, J., Wang, Z., Wang, J. & Wang, S. 2015 Improving the water flux and bio-fouling resistance of reverse osmosis (RO) membrane through surface modification by zwitterionic polymer. *Journal of Membrane Science* **493**, 188–199. https://doi.org/10.1016/j.memsci.2015.06.036.

Wei, X., Wang, Z., Zhang, Z., Wang, J. & Wang, S. 2010 Surface modification of commercial aromatic polyamide reverse osmosis membranes by graft polymerization of 3-allyl-5, 5-dimethyl hydantoin. *Journal of Membrane Science* **351**(1–2), 222–233. https://doi.org/10.1016/j.memsci.2010.01.054.

Xu, J., Wang, Z., Yu, L., Wang, J. & Wang, S. 2013 A novel reverse osmosis membrane with regenerable anti-biofouling and chlorine resistant properties. *Journal of Membrane Science* **435**, 80–91. https://doi.org/10.1016/j.memsci.2013.02.010.

Yu, S., Yao, G., Dong, B., Zhu, H., Peng, X. & Liu, J. 2013 Improving fouling resistance of thin-film composite polyamide reverse osmosis membrane by coating natural hydrophilic polymer sericin. *Separation and Purification Technology* **118**, 285–293. https://doi.org/10.1016/j.seppur.2013.07.018.

Yu, T., Meng, L., Zhao, Q., Shi, Y., Hu, H. & Lu, Y. 2017 Effects of chemical cleaning on RO membrane inorganic, organic and microbial foulant removal in a full-scale plant for municipal wastewater reclamation. *Water Research* **113**, 1–10. https://doi.org/10.1016/j.watres.2017.01.068.

Zhang, Z., Wang, Z., Wang, J. & Wang, S. 2013 Enhancing chlorine resistances and anti-biofouling properties of commercial aromatic polyamide reverse osmosis membranes by grafting 3-allyl-5, 5-dimethyl hydantoin and N,N′-Methylenebis (acrylamide). *Desalination* **309**, 187–196. https://doi.org/10.1016/j.desal.2012.10.019.

Zhang, T., Zhang, K., Li, J. & Yue, X. 2017 Simultaneously enhancing hydrophilicity, chlorine resistance and anti-biofouling of APA-TFC membrane surface by densely grafting quaternary ammonium cations and salicylaldimines. *Journal of Membrane Science* **528**, 296–302. https://doi.org/10.1016/j.memsci.2017.01.013.

Zhao, G. & Chen, W. 2015 Enhanced PVDF membrane performance via surface modification by functional polymer poly (N-isopropylacrylamide) to control protein adsorption and bacterial adhesion. *Reactive and functional Polymers* **97**, 19–29. https://doi.org/10.1016/j.reactfunctpolym.2015.10.001.

Zhao, Y., Song, L. & Leong, S. 2010 Fouling behaviour and foulant characteristics of reverse osmosis membranes for treated secondary effluent reclamation. *Journal of Membrane Science* **349**, 65–74. https://doi.org/10.1016/j.memsci.2009.11.023.